Title: Opposing effects of T cell receptor signal strength on CD4 T cells responding to acute versus chronic viral infection

Authors: Marco Künzli[1], Peter Reuther[2], Daniel D. Pinschewer[2], Carolyn G. King[1,3,*]

Affiliations:

[1]Immune Cell Biology Laboratory, Department of Biomedicine, University of Basel, University Hospital Basel CH-4031 Basel, Switzerland.

[2]Division of Experimental Virology, Department of Biomedicine – Haus Petersplatz, University of Basel, CH-4031 Basel, Switzerland.

[3]Lead contact

*Correspondence: carolyn.king@unibas.ch

To whom correspondence should be addressed:

Carolyn King
Department of Biomedicine
University of Basel
University Hospital Basel
Hebelstrasse 20
CH-4031 Basel, Switzerland
Email: carolyn.king@unibas.ch
Tel: +41 61 907 15 68

Abstract

A hallmark of the adaptive immune response is the ability of CD4 T cells to differentiate into a variety of pathogen appropriate and specialized effector subsets. A long-standing question in CD4 T cell biology is whether the strength of TCR signals can instruct one Th cell fate over another. The contribution of TCR signal strength to the development of Th1 and T follicular helper (Tfh) cells has been particularly difficult to resolve, with conflicting results reported in a variety of models. Although cumulative TCR signal strength can be modulated by the infection specific environment, whether or not TCR signal strength plays a dominant role in Th1 versus Tfh cell fate decisions across distinct infectious contexts is not known. Here we characterized the differentiation of CD4 TCR transgenic T cells responding to a panel of recombinant wild type or altered peptide ligand lymphocytic choriomeningitis viruses (LCMV) derived from acute and chronic parental strains. We found that while TCR signal strength positively regulates T cell expansion in both infection settings, it exerts opposite and hierarchical effects on the balance of Th1 and Tfh cells generated in response to acute versus persistent infection. The observation that weakly activated T cells, which comprise up to fifty percent of an endogenous CD4 T cell response, support the development of Th1 effectors highlights the possibility that they may resist functional inactivation during chronic infection. We anticipate that the panel of variant ligands and recombinant viruses described herein will be a valuable tool for immunologists investigating a wide range of CD4 T cell responses.

Keywords

T cell receptor signal, T cell receptor, T helper 1 cell, T follicular helper cell, infection, chronic infection, T cell exhaustion, T cell differentiation, CD4 T cell

Graphical abstract

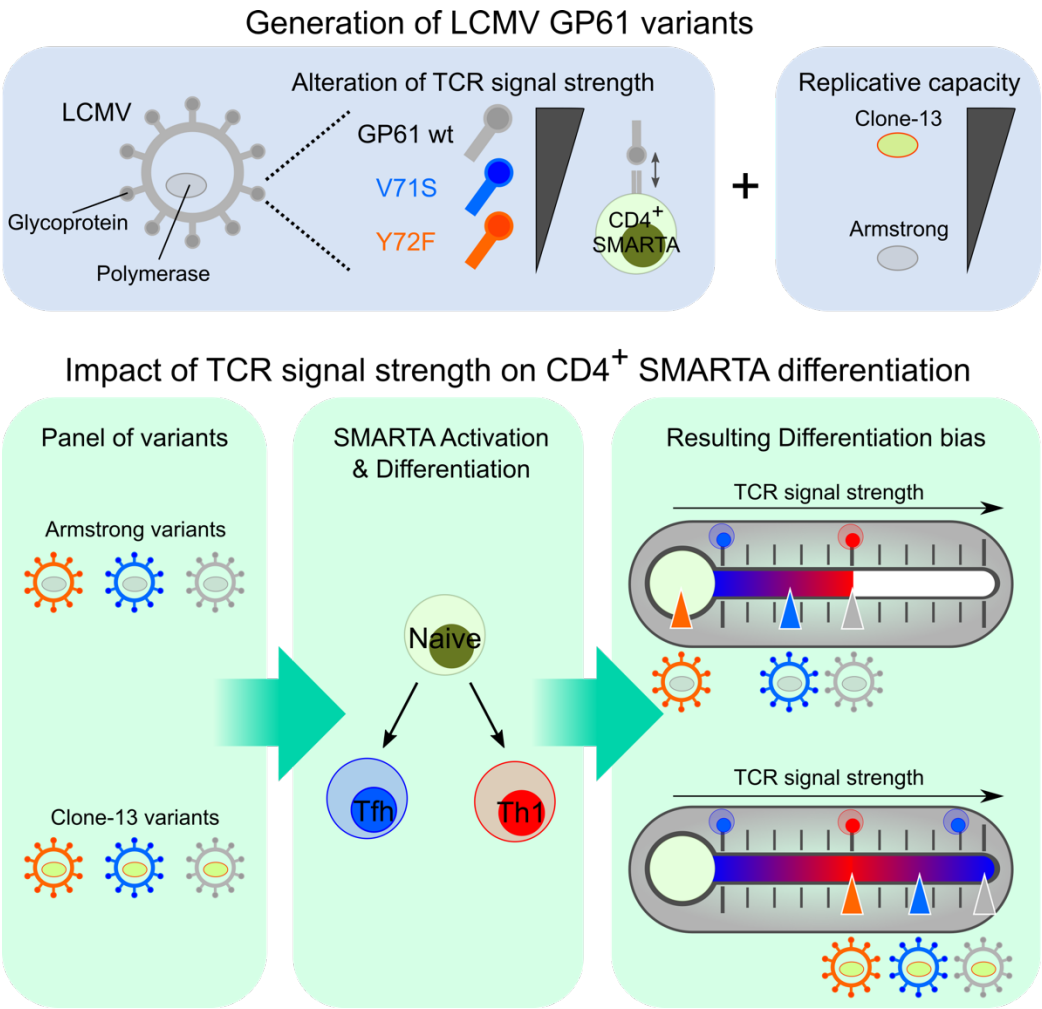

Highlights

- Identification of a wide panel of altered peptide ligands for the LCMV-derived GP61 peptide
- Generation of LCMV variant strains to examine the impact of TCR signal strength on CD4 T cells responding during acute and chronic viral infection
- The relationship between TCR signal strength and Th1 differentiation shifts according to the infection context: TCR signal strength correlates positively with Th1 generation during acute infection but negatively during chronic infection.

23 **Introduction**

24 Following infection or vaccination, antigen specific T cells undergo clonal
25 expansion and differentiation into effector cells with specialized functions. This
26 process begins with T cell receptor (TCR) recognition of peptide/MHC (pMHC) on
27 antigen presenting cells (APCs) and is further modulated by cytokines and
28 costimulatory molecules(*1, 2*). Viral infection induces the early bifurcation of CD4 T
29 cells into Th1 and T follicular helper (Tfh) cells. Th1 cells potentiate CD8 T cell and
30 macrophage cytotoxicity, whereas Tfh cells support antibody production by providing
31 survival and proliferation signals to B cells(*1, 3*).

32 Although the cumulative strength of interaction between TCR and pMHC has a
33 clear impact on T cell expansion and fitness, its influence on the acquisition of Th1
34 and Tfh cell fates is controversial(*4-12*). An essential role for TCR signal was
35 implicated in a study assessing the phenotype of progeny derived from individual, TCR
36 transgenic (tg) T cells responding during infection(*9*). The authors observed that
37 distinct TCRs induced reproducible and biased patterns of Th1 and Tfh phenotypes.
38 Although earlier reports suggested that Tfh cell differentiation requires high TCR signal
39 strength, recent work supports the idea that Tfh cells develop across a wide range of
40 signal strengths, while increasing TCR signal intensity favors Th1 generation(*4-11*). A
41 central difficulty in reconciling these findings is the use of different TCR tg systems as
42 well as immunization and infection models that may induce distinct levels of
43 costimulatory and inflammatory signals known to influence T cell differentiation.
44 Although existing reports suggest that persistent TCR signaling drives a shift towards
45 Tfh differentiation during chronic infection, whether this outcome can be modulated by
46 TCR signal strength has not been examined(*13-15*).

47 The impact of TCR signal strength on CD4 T cell differentiation *in vivo* has been
48 historically challenging to address. The use of MHC-II tetramers to track endogenous
49 polyclonal T cell responses does not adequately detect low affinity T cells that can
50 comprise up to fifty percent of an effector response in autoimmune or viral infection
51 settings(*16*). TCR tg models paired with a panel of ligands with varying TCR potency
52 have been informative, but only a handful of MHC-II restricted systems exist(*17, 18*).
53 To bypass these limitations, the generation of novel transgenic/retrogenic TCR strains
54 or recombinant pathogen strains is required(*4, 12, 19, 20*). To our knowledge, this
55 approach has not yet been used to modify a naturally occurring CD4 T cell epitope of
56 an infectious agent. To test the impact of TCR signal strength across different types
57 of infectious contexts, we generated a series of lymphocytic choriomeningitis virus
58 (LCMV) variants by introducing single amino acid mutations into the GP61 envelope
59 glycoprotein sequence and expressing them from both acute and chronic parent
60 strains. These strains were used to assess the dynamics and differentiation of
61 SMARTA T cells, a widely used TCR tg mouse line that mirrors the endogenous,
62 immunodominant CD4 T cell response to LCMV(*13*). We observed that depending on
63 the infection setting, TCR signal strength has opposing effects on the balance between
64 Th1 and Tfh cell differentiation. In an acute infection, strong TCR signals preferentially
65 induce Th1 effectors, whereas weak TCR signals shift the balance toward Tfh
66 effectors. In contrast, strong T cell activation during chronic infection induces Tfh cell
67 differentiation while more weakly activated T cells are biased to differentiate into Th1
68 cells. Based on these findings we propose a Goldilocks model for the generation of
69 Th1 effectors during viral infection, where too little or too much TCR signaling skews
70 the CD4 T cell response toward Tfh differentiation.

71 **Results**

72 ***Generation and viral fitness of GP61 LCMV variants***

73 To generate recombinant LCMV variants, we first screened a panel of altered
74 peptide ligands (APLs) with single amino acid mutations in the LCMV derived GP61
75 peptide. Using the early activation marker CD69 as a proxy for TCR signal strength
76 we identified 75 APLs for the SMARTA TCR transgenic line (Figure S1A, Figure 1A,
77 B, Table 1). We selected twelve of these APLs, covering a wide range of T cell
78 activation potential, to generate recombinant variant viruses, using site-directed PCR
79 mutagenesis (*21*). Five APL-encoding sequences were successfully introduced into
80 the genomes of both LCMV Armstrong (Armstrong variants) and Clone-13 (Clone-13
81 variants), the latter of which contains a mutation in the polymerase gene L that
82 enhances the replicative capacity of the virus, enabling viral persistence(*22, 23*). To
83 exclude a potential impact of differential glycoprotein-mediated viral tropism on CD4
84 T cell differentiation, we equipped both the Armstrong- and Clone-13-based viruses
85 with the identical glycoprotein of the WE strain and introduced the epitope mutations
86 therein (resulting viruses referred to as rLCMV Armstrong and rLCMV Clone-13,
87 respectively)(*24*). Of these viruses, two variants, V71S and V72F (EC50 ~ 0.1 μM and
88 1μM, respectively) demonstrated comparable viral fitness *in vitro* and *in vivo* (Figure
89 1C, D). We further performed an out-competition assay with invariant chain knockout
90 splenocytes to ensure comparable presentation of these APLs by MHC-II (Figure
91 1E)(*25*). Taken together, these data demonstrate the development of a novel tool to
92 examine the impact of TCR signal strength on SMARTA T cells activated by either
93 acute or chronic viral infection.

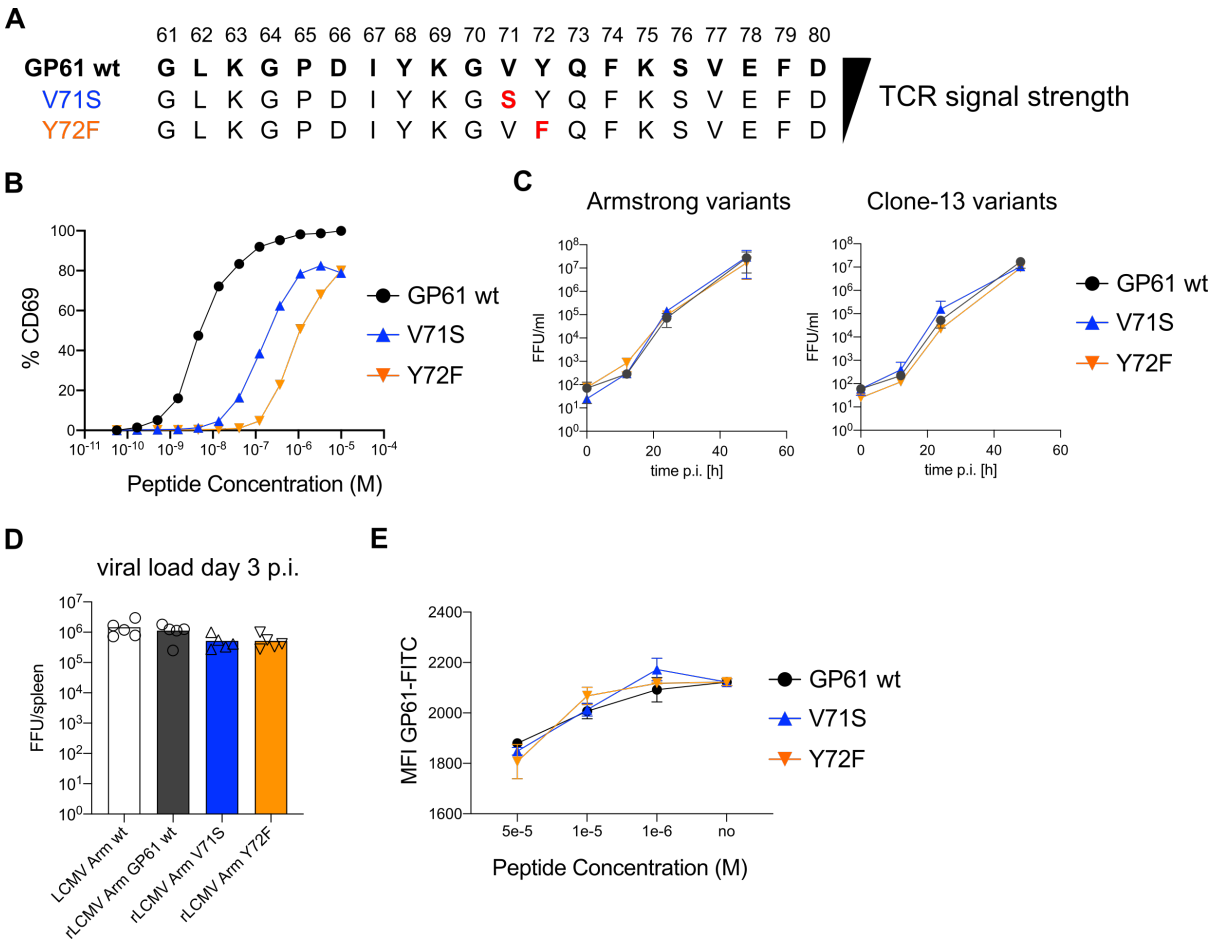

Figure 1: Generation and viral fitness of GP61 LCMV variants
(A) Scheme of GP61 wt and APL sequences with mutations highlighted in red ordered hierarchically according to TCR signal strength.
(B) Peptide dose – activation curves of overnight cultured SMARTA cells with peptide pulsed splenocytes using the percentage of CD69$^+$ SMARTA cells as a readout for activation. EC_{50} values are ~ 5 nM for GP61 wt, ~ 0.1 µM for V71S and ~ 1µM for Y72F.
(C) *In vitro* growth kinetics depicting the viral load in the culture medium (FFU/ml, focus forming units) of GP61 wt or V71S and Y72F variants of Armstrong (left) and Clone-13 (right) variant infection on BHK21 cells over time. Data are displayed as mean ± SD.
(D) Early splenic viral load day 3 post infection (p.i.) in Armstrong variants. Bars represent the mean and symbols represent individual mice.
(E) Peptide dose – response curves depicting the out-competition of the GP61 FITC signal by unlabeled GP61 wt or variants on B220$^+$ B cells. Data are displayed as mean ± SD of 2-3 technical replicates.
Data represent one of n = 2 independent experiments (B, D-,E) or pooled data from n = 2 independent experiments (C).

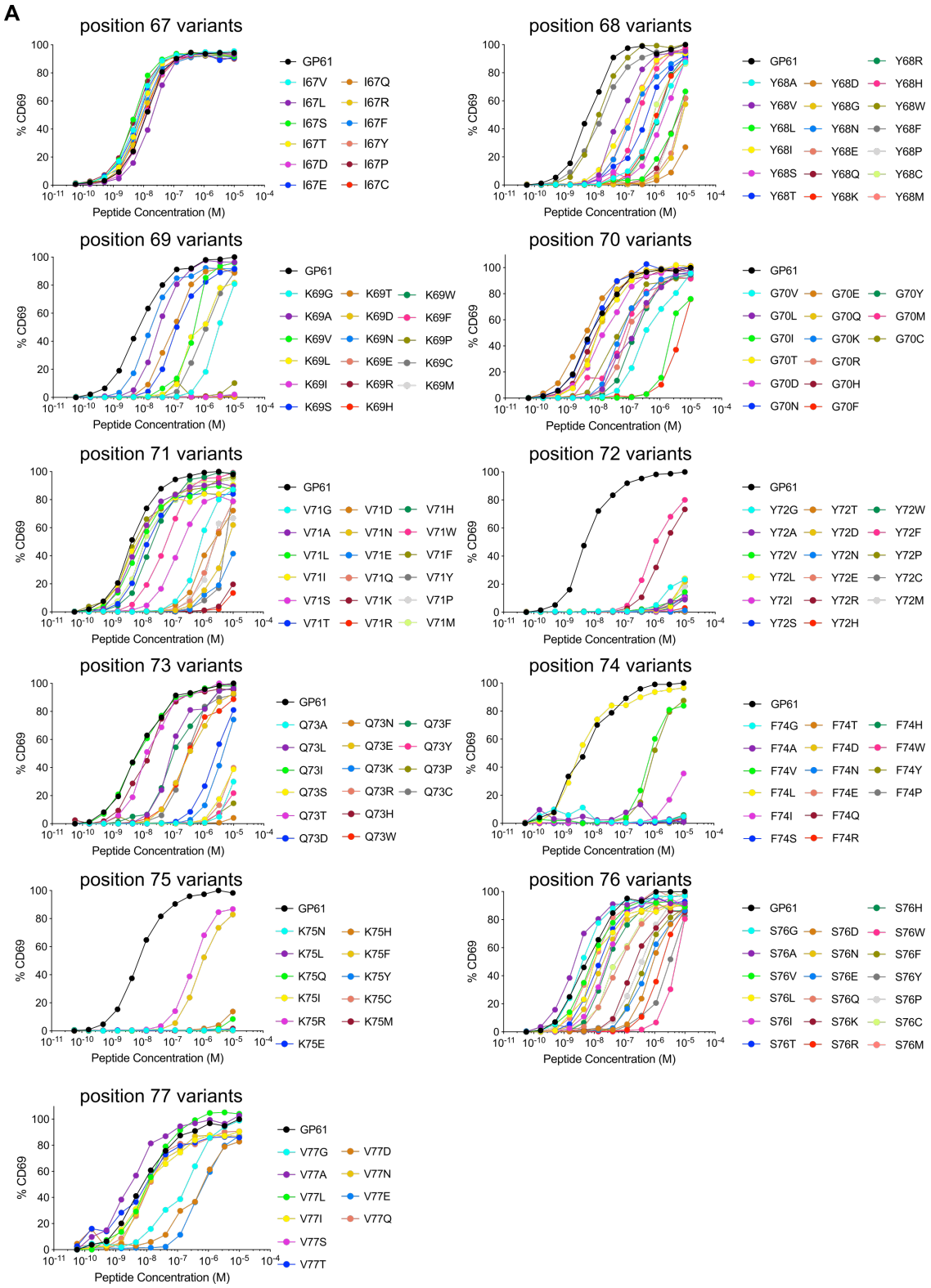

Figure S1: Generation and viral fitness of GP61 LCMV variants

(A) Peptide dose – activation curves of overnight cultured SMARTA cells with peptide pulsed splenocytes using the percentage of CD69⁺ SMARTA cells as a readout for activation.

Data represent one of n = 2 independent experiments.

APL	EC50 [M]
GP61wt	5.2E-09
Y68 A	1.3E-06
Y68 V	7.2E-08
Y68 L	6.5E-06
Y68 I	1.3E-07
Y68 S	2.6E-06
Y68 T	4.8E-07
Y68 N	1.6E-07
Y68 E	7.0E-05
Y68 Q	6.7E-06
Y68 K	1.1E-06
Y68 R	1.5E-06
Y68 H	3.1E-07
Y68 W	1.4E-08
Y68 P	1.1E-05
Y68 C	1.0E-06
Y68 M	1.6E-07
K69 G	5.2E-06
K69 A	3.2E-08
K69 V	5.0E-07
K69 L	5.5E-07
K69 S	1.2E-07
K69 T	8.1E-08
G70 V	3.5E-07
G70 L	1.2E-07
G70 I	3.5E-06
G70 K	5.8E-08
G70 R	1.1E-07
G70 F	1.4E-05
G70 Y	1.7E-07
G70 M	6.2E-08
V71 G	9.3E-07
V71 S	1.4E-07
V71 D	1.4E-06
V71 N	8.4E-06
V71 E	9.5E-06
V71 Q	2.9E-06
V71 H	2.2E-08

APL	EC50 [M]
V71 W	5.9E-08
V71 P	2.2E-06
V71 M	1.2E-08
V71 C	2.1E-07
Y72 S	4.2E-05
Y72 T	1.7E-05
Y72 E	2.1E-07
Y72 R	2.1E-06
Y72 F	9.6E-07
Y72 P	6.3E-08
Y72 M	5.6E-05
Q73 L	8.7E-08
Q73 S	2.5E-05
Q73 D	3.2E-06
Q73 E	3.1E-07
Q73 K	8.3E-06
Q73 W	2.6E-07
Q73 F	1.1E-07
Q73 C	2.9E-07
F74 V	8.7E-07
F74 I	1.9E-05
F74 Y	1.3E-06
K75 R	5.1E-07
S76 D	1.0E-06
S76 E	5.7E-07
S76 Q	5.9E-08
S76 K	2.0E-07
S76 R	2.2E-06
S76 W	7.9E-05
S76 F	4.5E-07
S76 Y	5.3E-06
S76 P	3.8E-07
S76 C	5.9E-08
V77 G	1.8E-07
V77 S	3.6E-08
V77 D	4.8E-07
V77 E	6.5E-07
V77 P	4.0E-08

Table 1: APLs with altered potential to activate SMARTA and corresponding EC_{50} values.

94 ***TCR signal strength positively correlates with Th1 cell differentiation during***
95 ***LCMV Armstrong variant infection***

96 To assess the impact of TCR signal strength during acute viral infection,
97 SMARTA T cells were transferred into congenic recipients followed by infection with
98 rLCMV Armstrong GP61 wt, V71S or Y72F. All LCMV variants were capable of
99 inducing SMARTA T cell expansion at day 10 post infection (p.i.) and a direct
100 correlation between TCR signal strength and the number of SMARTA T cells
101 recovered was observed (Figure 2A). In contrast, expansion of endogenous LCMV
102 nucleoprotein (NP)-specific as well as antigen-experienced $CD44^+$ T cells was similar
103 across all three viral strains (Figure 2A). The expansion hierarchy among the viruses
104 was maintained >30 days after LCMV infection (Figure 2A).

105 We next examined the phenotype of SMARTA T cells, focusing our analyses
106 on effector cells due to the impaired generation of Tfh memory by SMARTA T
107 cells(*26*). As the Y72F variant induced very few effector cells, we excluded this strain
108 from further investigation. Consistent with earlier reports, strong T cell stimulation
109 induced a larger proportion of $Ly6c^+$ Th1 effectors, whereas the proportion of Tfh
110 effectors was decreased (Figure 2B-D)(*4, 8-10*). In contrast, the ratio of Th1 and Tfh
111 effector cells generated by host NP-specific T cells was consistent across all viral
112 strains, providing an internal control for the comparable ability of these viruses to
113 induce endogenous T cell responses (Figure 2D, Figure S2A). Expression of folate
114 receptor 4 (FR4), an alternative marker for Tfh cell identification, was additionally used
115 in combination with PD1 to discriminate the Tfh cell compartment, and demonstrated
116 a decreased proportion of Tfh cells activated by strong compared to weak TCR
117 stimulation (Fig. S2B)(*26, 27*). Accordingly, the expression of Bcl6 and T-bet, lineage
118 defining transcription factors for Tfh and Th1 cells, respectively, revealed a mild but

119 significant trend toward increased Tbet and decreased Bcl6 in response to strong
120 stimulation (Fig. 2E). Importantly, Bcl6 expression was higher on Tfh compared to
121 Th1 effectors, with no differences observed between strong and weak stimulation
122 (Figure 2F, S2C). These data indicate that TCR signal strength is unlikely to exert a
123 qualitative impact on these subsets. Notably, we did not observe any impact of TCR
124 signal strength on the development of PSGL1^{hi}Ly6c^{lo} T cells, previously reported to be
125 a less differentiated population of Th1 effectors (Figure S2D)(*26*). In sum, consistent
126 with earlier reports, TCR signal strength positively correlates with an increased ratio
127 of Th1 to Tfh effectors during acute LCMV infection.

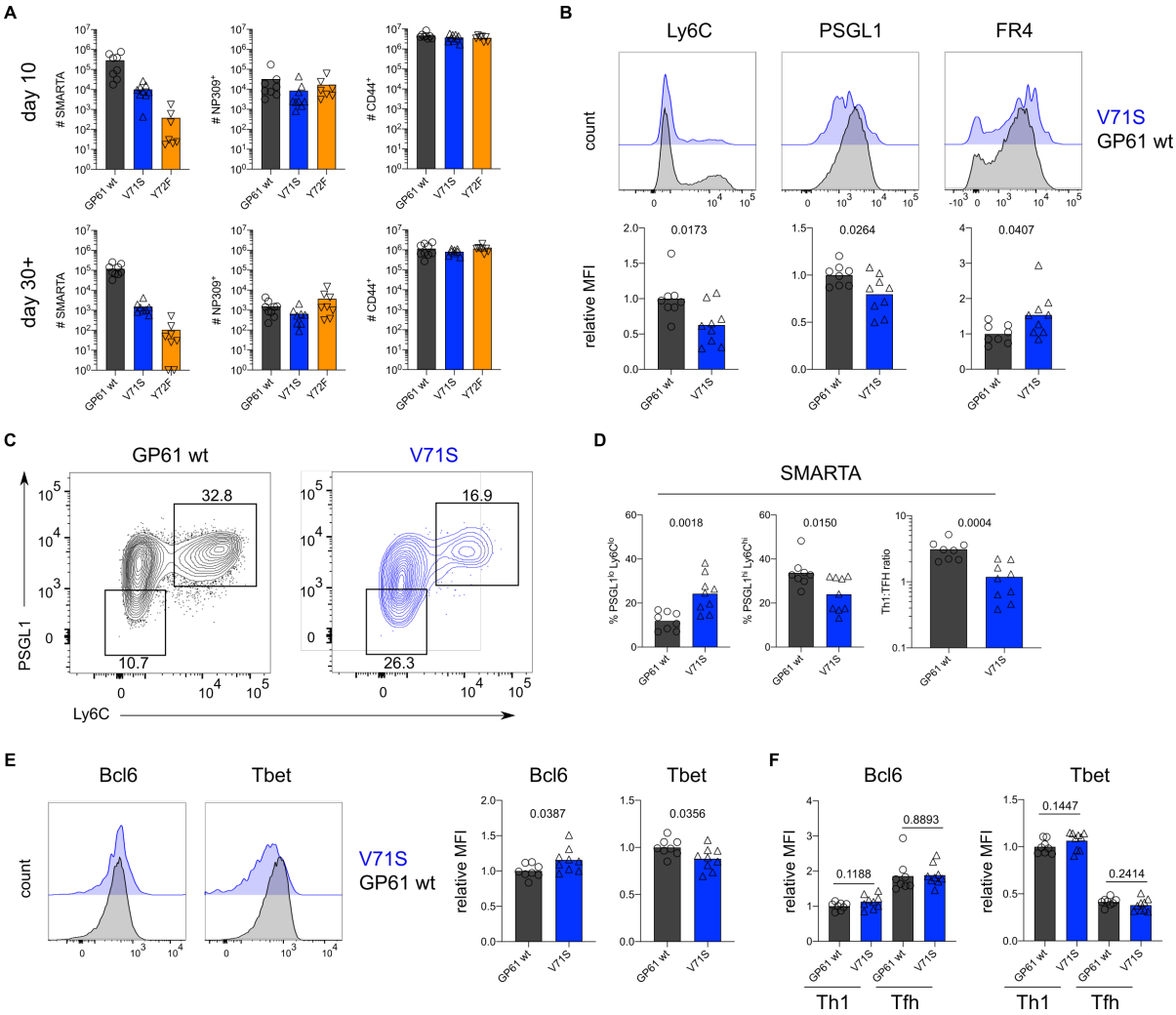

Figure 2: TCR signal strength positively correlates with Th1 cell differentiation during LCMV Armstrong variant infection

(A) Number of SMARTA (left), NP309^{+} (middle) and CD44^{+} cells (right) 10 days (top) or >30 days (bottom) p.i.

(B) Histograms (top) and relative MFI (bottom) of indicated phenotypic markers in the SMARTA compartment 10 days p.i.

(C) Identification of Th1 (Ly6C^{hi}PSGL1^{hi}) and Tfh (Ly6C^{lo}PSGL1^{lo}) subset in the SMARTA compartment by flow cytometry 10 days p.i.

(D) Proportion of Tfh (left), Th1 cells (middle) and the Th1:Tfh ratio (right) of the SMARTA compartment 10 days p.i.

(E) Histograms (left) and relative MFI (right) of Bcl6 and Tbet expression in the SMARTA compartment 10 days p.i

(F) Bcl6 and Tbet MFI in SMARTA Th1 and Tfh subsets.

Data are pooled from n = 2 independent experiments with 7-9 samples per group. Bars represent the mean and symbols represent individual mice. Significance was determined by unpaired two-tailed Student's t-tests.

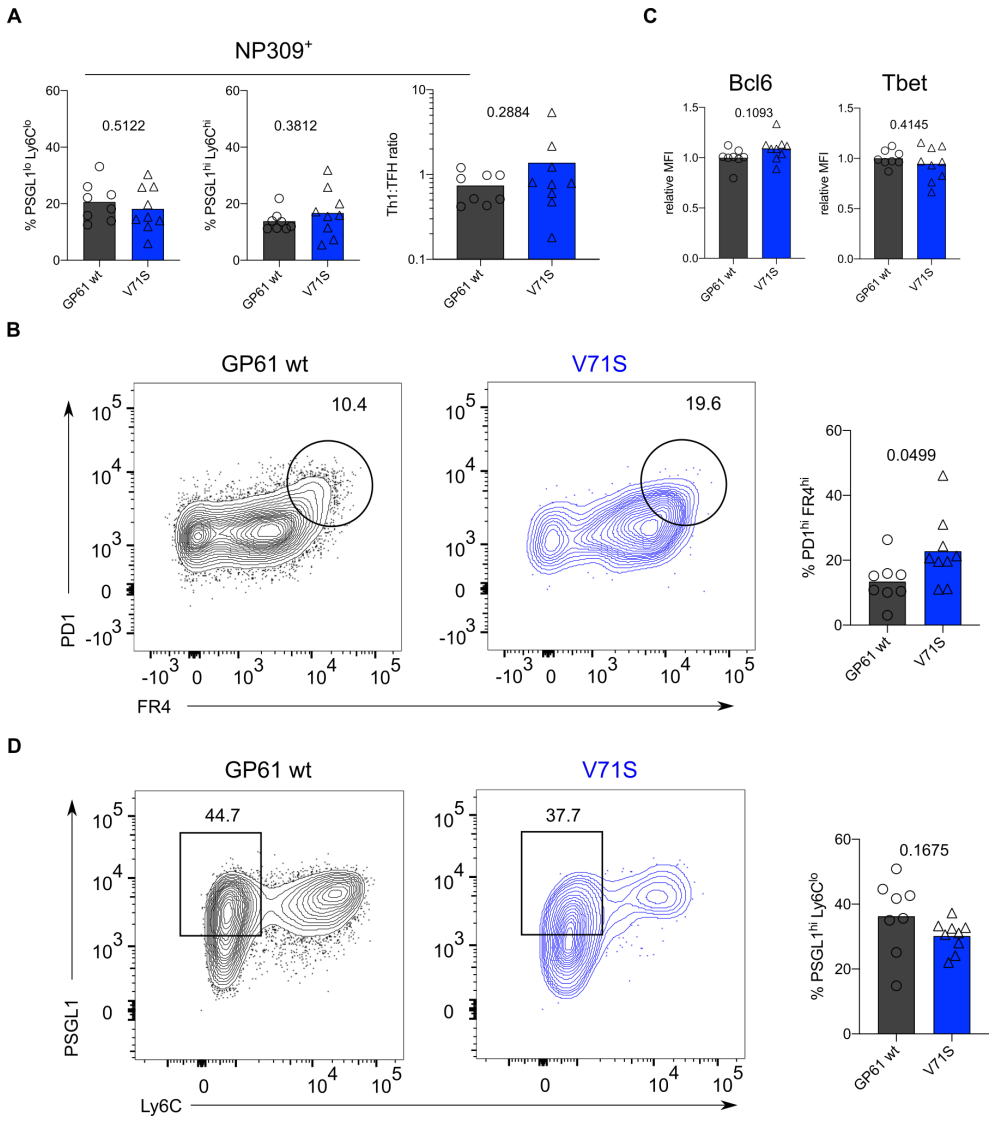

Figure S2: TCR signal strength positively correlates with Th1 cell differentiation during LCMV Armstrong variant infection

(A) Proportion of Tfh (left), Th1 cells (middle) and the Th1:Tfh ratio (right) of the NP309^{+} compartment 10 days p.i.

(B) Identification and proportion of PD1^{hi} FR4^{hi} Tfh cells in the SMARTA compartment by flow cytometry.

(C) Relative MFI of Bcl6 and Tbet expression in the Ly6C^{lo} Th1 SMARTA compartment.

(D) Identification and proportion of Ly6C^{lo} Th1 (Ly6C^{lo}PSGL1^{hi}) in the SMARTA compartment by flow cytometry.

Data are pooled from n = 2 independent experiments with 8-9 samples per group. Bars represent the mean and symbols represent individual mice. Significance was determined by unpaired two-tailed Student's t-tests.

128 ***TCR signal strength positively correlates with Tfh cell differentiation during***
129 ***LCMV Clone-13 variant infection***

130 In contrast to acute LCMV infection, SMARTA T cells responding to chronic
131 LCMV preferentially adopt a Tfh effector phenotype(*14, 15*). The impact of TCR signal
132 strength within this context has not been determined, although affinity diversity among
133 endogenous T cells is reportedly similar between acute and chronic LCMV
134 infection(*28*). To directly assess the impact of TCR signal strength during chronic
135 infection we transferred SMARTA T cells into congenic recipients followed by infection
136 with rLCMV Clone-13 expressing either GP61 wt, V71S or Y72F. As an additional
137 control we infected mice with rLCMV Armstrong which induced a similar expansion of
138 SMARTA, NP-specific and $CD4^{+}CD44^{+}$ T cells as its Clone-13 counterpart (Fig S3A).
139 Consistent with the results from acute infection, SMARTA T cell numbers at day 7 p.i.
140 positively correlated with TCR signal strength, while the expansion of NP-specific and
141 $CD4^{+}CD44^{+}$ T cells was similar in response to all three Clone-13 variants (Figure 3A).
142 Importantly, infection with rLCMV Clone-13 Y72F induced approximately 2-fold more
143 SMARTA T cell effectors compared to acute infection, allowing for a thorough
144 investigation of T cells responding to this very weak potency variant (Figure 3A, Figure
145 2A).

146 With respect to T cell phenotype, strong TCR stimulation during rLCMV Clone-
147 13 GP61 wt infection shifted the balance toward Tfh effector cell differentiation when
148 compared to strong TCR stimulation in the context of acute infection (Figure S3B-C).
149 Unexpectedly, and in contrast to the Armstrong variants, weaker TCR signaling during
150 Clone-13 variant infection resulted in increased proportions of both $PSGL1^{hi}Ly6c^{hi}$ and
151 $PSGL1^{hi}Ly6c^{lo}$ Th1 cells with the weakest variant, Y72F, generating the highest
152 proportion of Th1 effectors (Figure 3B-D, S3D). The shift toward Th1 effectors in

153 response to lower TCR signal strength is unlikely due to differences in antigen load as
154 all variants sustained high viral titers in the kidneys at day 7 p.i (Figure S3E). In
155 addition, although the viral titer of intermediate potency variant V71S was slightly
156 decreased compared to GP61 wt and Y72F infection, NP-specific CD4 T cells
157 exhibited a similar ratio of Th1 to Tfh effectors across all three infections (Figure S3F).
158 Taken together, these reveal that TCR signal strength differentially modulates T cell
159 fate acquisition according to the infectious context.

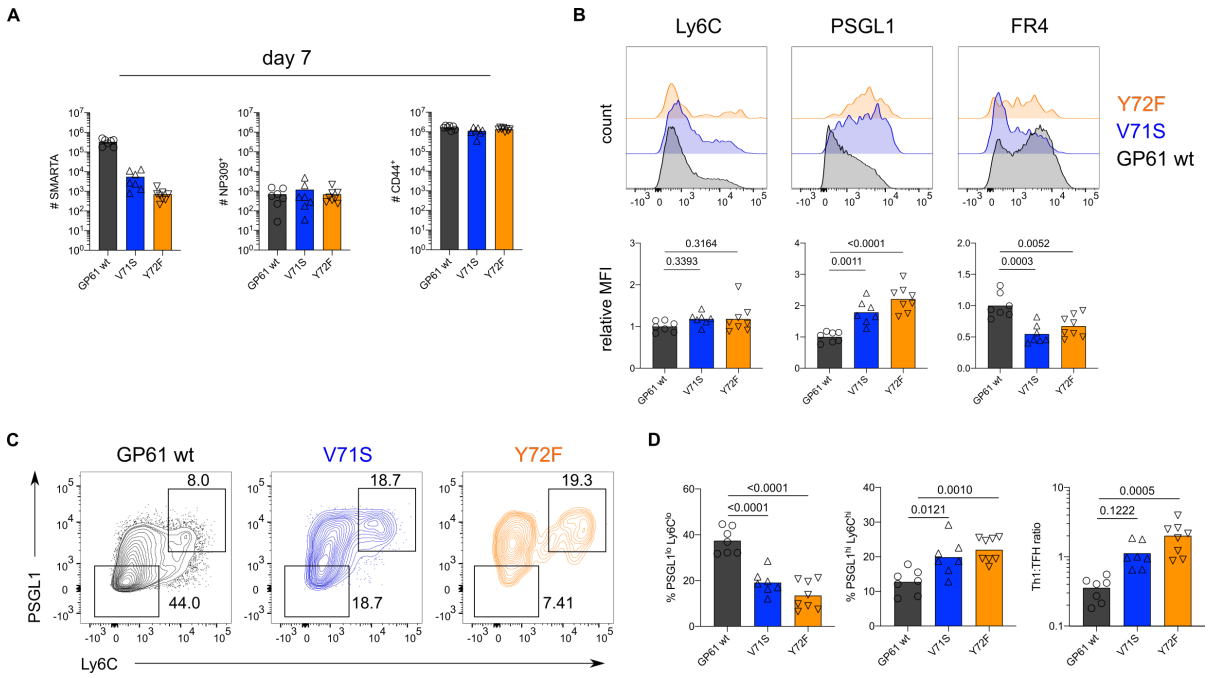

Figure 3: TCR signal strength positively correlates with Tfh cell differentiation during LCMV Clone-13 variant infection

Spleens were harvested 7 days after infection with LCMV Clone-13 variants.
(A) Number of SMARTA (left), NP309^{+} (middle) and CD44^{+} cells (right).
(B) Histograms (top) and relative MFI (bottom) of indicated phenotypic markers in the SMARTA compartment.
(C) Identification of Th1 (Ly6C^{hi}PSGL1^{hi}) and Tfh (Ly6C^{lo}PSGL1^{lo}) subset in the SMARTA compartment by flow cytometry.
(D) Proportion of Tfh (left), Th1 cells (middle) and the Th1:Tfh ratio (right) of the SMARTA compartment.
Data are pooled from n = 2 independent experiments with 7-8 samples per group. Bars represent the mean and symbols represent individual mice. Significance was determined by one-way analysis of variance (ANOVA) followed by Tukey's post-test.

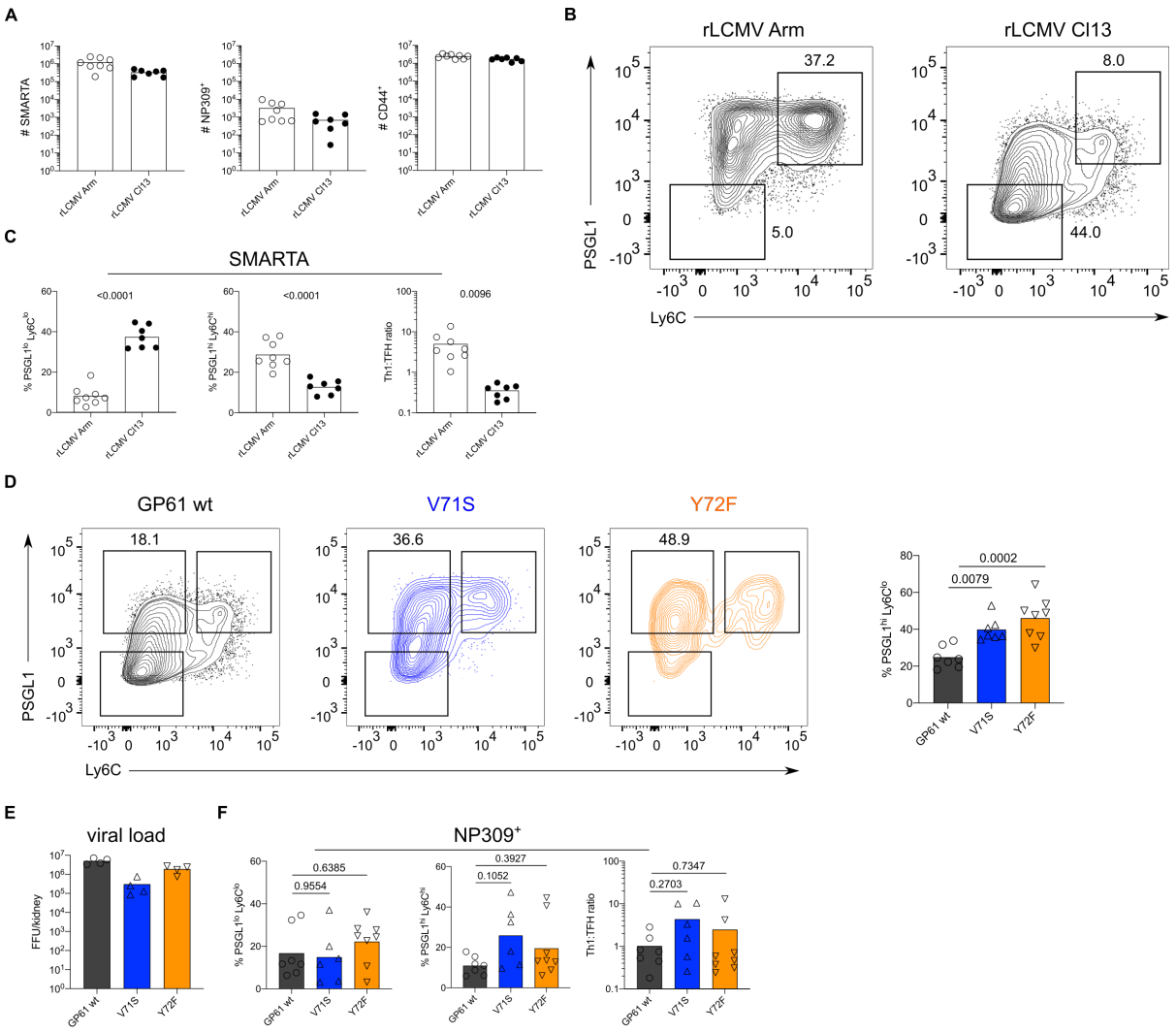

Figure S3: TCR signal strength positively correlates with Tfh cell differentiation during LCMV Clone-13 variant infection

Spleens were harvested 7 days after infection with LCMV Clone-13 variants.

(A) Number of SMARTA (left), NP309^{+} (middle) and CD44^{+} cells (right).

(B) Identification of Th1 (Ly6C^{hi}PSGL1^{hi}) and Tfh (Ly6C^{lo}PSGL1^{lo}) subset in the SMARTA compartment by flow cytometry.

(C) Proportion of Tfh (left), Th1 cells (middle) and the Th1:Tfh ratio (right) of the SMARTA compartment.

(D) Identification and proportion of Ly6C^{lo} Th1 (Ly6C^{lo}PSGL1^{hi}) in the SMARTA compartment by flow cytometry.

(E) Viral load in kidneys.

(F) Proportion of Tfh (left), Th1 cells (middle) and the Th1:Tfh ratio (right) of the NP309^{+} compartment.

Data are pooled from n = 2 independent experiments with 7-8 samples per group except for (E) where one representative experiment of n = 2 independent experiments is shown with 4 samples per group. Bars represent the mean and symbols represent individual mice. Significance was determined by one-way analysis of variance (ANOVA) followed by Tukey's post-test.

160 ***Increasing TCR signal strength promotes the expression of markers***
161 ***associated with chronic T cell stimulation***

162 During Clone-13 infection, T cells start to upregulate inhibitory surface markers
163 associated with chronic activation, a state often referred to as "exhaustion"(*15, 29-31*).
164 To understand if TCR signal strength impacts the expression of these markers we
165 analyzed SMARTA T cells responding to Clone-13 GP61 wt and variant viruses at day
166 14. T cells responding to strong TCR signals expressed the highest levels of both
167 PD1 and Lag3, two well characterized co-inhibitory receptors (Figure 4A-B) (*15, 29*).
168 SMARTA T cells co-expressing both PD1 and Lag3 were most abundant following
169 Clone-13 GP61 wt infection and decreased in response to Clone-13 variant infection
170 (Figure 4C-D). Although the viral load was decreased in Clone-13 variant infections
171 at this time point, the basal activation of $CD4^+CD44^+$ T cells was equivalent across all
172 three strains and clearly above the recombinant LCMV Armstrong control (Figure S4A-
173 B). Next, we examined the expression of TOX, a transcription factor involved in the
174 adaptation of CD8 T cells to chronic infection(*32-36*). In response to acute infection,
175 SMARTA Tfh cells expressed higher levels of TOX compared to Th1 cells, consistent
176 with an earlier study highlighting the importance of TOX for Tfh cell development
177 (Figure S4C)(*37*). In contrast, TOX expression during rLCMV Clone-13 wt infection
178 was most highly upregulated by Th1 effectors (Figure S4C). In line with the expression
179 of PD1 and Lag3, TOX was decreased on SMARTA T cells responding to rLCMV
180 Clone-13 variant viruses, despite being comparably induced on $CD4^+CD44^+$ T cells
181 (Figure 4E, Figure S4D). TOX was recently demonstrated to be important for the
182 survival of stem-like $TCF1^+$ CD8 T cells that accumulate during chronic LCMV(*34, 38,*
183 *39*). Given the transcriptional similarities of $TCF1^+$ CD8 T cells and Tfh cells, we
184 wondered if TCF1 would be similarly regulated by TCR signal strength following Clone-

185 13 variant infection(*40*). Here we observed that unlike TOX expression, TCF1 is
186 similarly expressed by T cells responding to all three rLCMV Clone-13 variants (Figure
187 4F, S4E), indicating that TCF1 expression is likely to be maintained independently of
188 TCR signals.

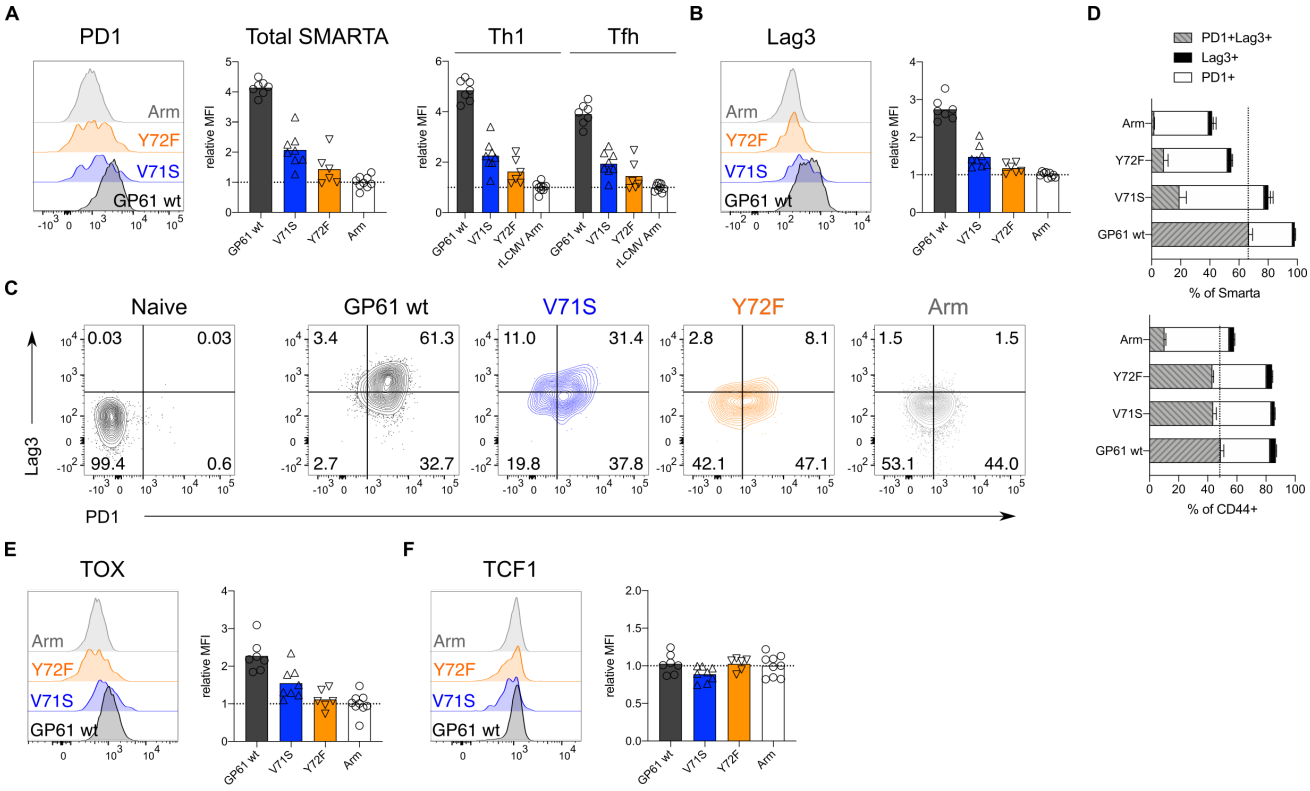

Figure 4: Increased TCR signal strength induces expression of markers associated with chronic T cell stimulation

Spleens were harvested 14 days after infection with LCMV Clone-13 based variants.
(A) Histograms (left) and relative MFI (right) of PD1 in the total SMARTA compartment (left) or SMARTA Th1 and Tfh subsets (right).
(B) Histograms (left) and relative MFI (right) of Lag3 in the SMARTA compartment.
(C) Identification of PD1^{+}Lag3^{+} SMARTA cells by flow cytometry compared to naïve CD62L^{+} CD44^{-} CD4 T cells from an uninfected mouse.
(D) Quantification of PD1^{+}Lag3^{+} SMARTA cells in the SMARTA (top) or CD44^{+} (bottom) compartment.
(E) Histogram (left) and relative MFI (right) of TOX in the SMARTA compartment.
(F) Histogram (left) and relative MFI (right) of TCF1 in the SMARTA compartment.
Data are pooled from n = 2 independent experiments with 6-9 samples per group. Bars represent the mean and symbols represent individual mice. Significance was determined by one-way analysis of variance (ANOVA) followed by Tukey's post-test.

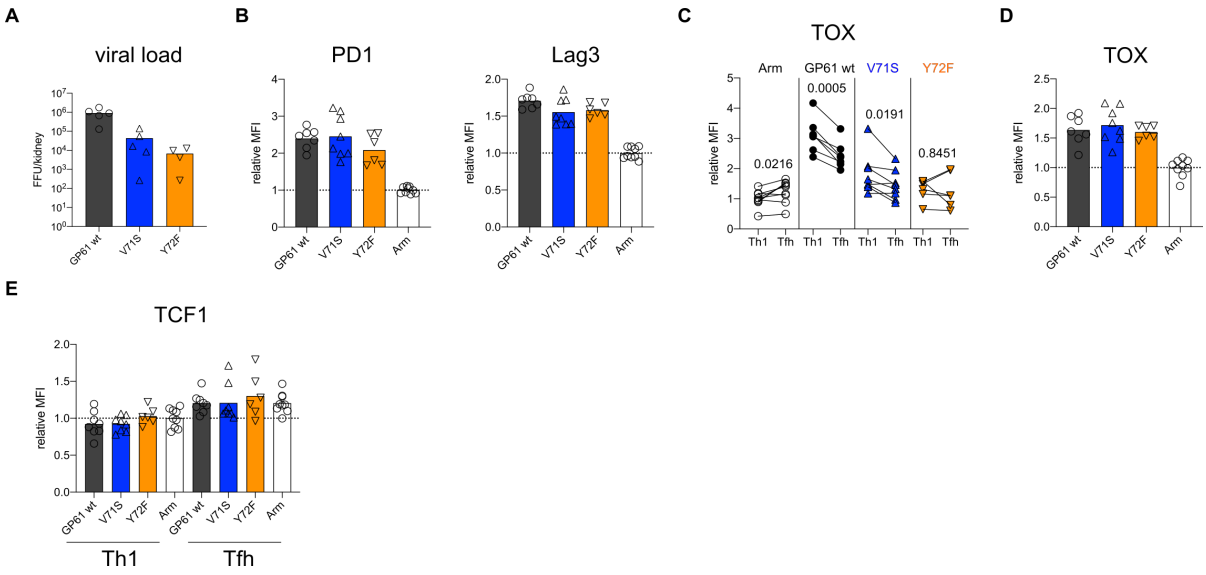

Figure S4: Increased TCR signal strength induces expression of markers associated with chronic T cell stimulation

Spleens were harvested 14 days after infection with LCMV Clone-13 based variants.
(A) Viral load in kidneys.
(B) Relative MFI (right) of PD1 and Lag3 in the CD44$^+$ compartment.
(C) Relative MFI of TOX in SMARTA Th1 and Tfh.
(D) Relative MFI (right) of TOX in the CD44$^+$ compartment.
(E) Relative MFI of TCF1 in the SMARTA Th1 and Tfh subsets.
Data are pooled from n = 2 independent experiments with 6-9 samples per group except for (A) where one representative experiment of n = 2 independent experiments is shown with 4-5 samples per group. Bars represent the mean and symbols represent individual mice. Significance was determined by one-way analysis of variance (ANOVA) followed by Tukey's post-test (B,D) or by paired two-tailed Student's t-tests (C).

189 **Discussion**

190 The results of this study highlight the differential impact of TCR signal strength
191 in shaping CD4 T cell fate according to the infection context. By systematically
192 comparing the differentiation of TCR transgenic T cells responding to variant ligands
193 in two distinct infection models, we demonstrate that the impact of TCR signal strength
194 is heavily dependent on the infection specific parameters such as antigen load and
195 inflammation.

196 The observation that TCR signal intensity correlates with Th1 generation during
197 acute infection is consistent with accumulating evidence that higher potency ligands
198 increase T cell sensitivity to IL-2, which likely drives the survival and expansion of Th1
199 effectors (*4, 8, 41-45*). This is similar to the paradigm described for Th1/Th2 cell
200 differentiation, where stronger signals induce Th1 cells and weaker signals induce Th2
201 cells(*46*). Nevertheless, at very high antigen doses, T cells revert to Th2
202 differentiation, potentially due to the susceptibility of Th1 cells to activation induced
203 cell death (AICD)(*47, 48*). AICD of Th1 cells might also contribute to biased Tfh
204 generation at the higher end of TCR signal strength during Clone-13 infection(*49, 50*).

205 The shift of relatively high affinity CD4 T cells toward a Tfh cell phenotype
206 during Clone-13 infection is well documented(*14, 40, 51*). In addition to antigen
207 persistence, however, Clone-13 presents an altered inflammatory environment which
208 contributes to an interferon stimulated gene signature and IL-10 production by
209 chronically activated CD4 T cells(*15, 52*). It is possible that the unique cytokine milieu
210 present during Clone-13 infection cooperates with strong TCR signals to fine tune T
211 cell fate. For example, activation of T cells in the presence of IFNα induces T cell
212 secretion of IL-10 which is positively regulated by TCR signal strength(*53, 54*). While
213 this may ultimately serve to limit host pathology, it may also prevent the accumulation

214 of Th1 effectors. Consistent with this idea, blocking IFNα or IL-10 during Clone-13
215 infection rescues the Th1 effector compartment and improves viral control, although
216 this likely depends on the rate of viral replication(*55-57*). Within the same
217 inflammatory context, weaker TCR signals might induce less T cell derived IL-10 which
218 has been shown to impair Th1 effector cell differentiation(*52*). Of particular interest, T
219 cell production of IL-10 during chronic infection depends on sustained, but ERK-
220 independent TCR signals, suggesting that inflammatory versus suppressive cytokine
221 secretion may have distinct TCR signaling requirements(*52*). Future experiments
222 should address this by determining whether TCR signal strength contributes to
223 cytokine production as well as cytokine susceptibility (i.e. induction of cytokine
224 receptors) of effector cells responding during acute and chronic viral infection.
225 Finally, the ability of weakly activated T cells to maintain a higher proportion of
226 Th1 effectors might ultimately contribute to viral control. The observation that the
227 weakest Clone-13 variant, Y72F, elicited significantly more expansion than its
228 Armstrong counterpart demonstrates that prolonged antigen presentation supports the
229 accumulation of relatively low affinity T cells. Importantly, our study only follows the
230 differentiation of T cells specific for a single epitope, while low affinity T cells are
231 demonstrated to comprise up to half of the endogenous effector T cell response(*58*).
232 Going forward, it will be interesting to determine whether targeting the expansion of
233 lower affinity T cells with the potential to resist functional inactivation and maintain
234 proliferative potential will improve control of viral infection.
235
236 **Acknowledgments**
237 We thank all members of the Pinschewer lab for helpful discussion and David
238 Schreiner for editing of the manuscript. Research was supported by the Swiss

National Science Foundation (SNF, grants number PP00P3_157520 to CGK and number 310030_173132 to DDP), Gottfried and Julia Bangerter-Rhyner Stiftung, Olga Mayenfisch Stiftung, the Nikolaus and Bertha Burckhardt-Bürgin Stiftung (NBB), and the Freiwillige Akademische Gesellschaft (FAG) Basel.

Author contributions

C.G.K. conceptualized the project. M.K. and C.G.K. designed the experiments, analyzed the data, wrote the manuscript and acquired funding. M.K. and P.R. performed experiments. D.P. acquired funding, provided advice on experimental design and revised the manuscript.

Declaration of Interests

The authors declare no competing interests.

References

252 1. J. Zhu, H. Yamane, W. E. Paul, Differentiation of effector CD4 T cell populations (*).
253 *Annu Rev Immunol* **28**, 445-489 (2010).
254 2. M. M. Davis *et al.*, Ligand recognition by alpha beta T cell receptors. *Annu Rev*
255 *Immunol* **16**, 523-544 (1998).
256 3. S. Crotty, Follicular Helper CD4 T Cells (TFH). *Annual Review of Immunology* **29**, 621-
257 663 (2011).
258 4. S. Keck *et al.*, Antigen affinity and antigen dose exert distinct influences on CD4 T-cell
259 differentiation. *Proc Natl Acad Sci U S A* **111**, 14852-14857 (2014).
260 5. D. I. Kotov *et al.*, TCR Affinity Biases Th Cell Differentiation by Regulating CD25,
261 Eef1e1, and Gbp2. *J Immunol* **202**, 2535-2545 (2019).
262 6. J. P. Snook, C. Kim, M. A. Williams, TCR signal strength controls the differentiation of
263 CD4(+) effector and memory T cells. *Sci Immunol* **3**, (2018).
264 7. D. DiToro *et al.*, Differential IL-2 expression defines developmental fates of follicular
265 versus nonfollicular helper T cells. *Science* **361**, (2018).
266 8. V. Krishnamoorthy *et al.*, The IRF4 Gene Regulatory Module Functions as a Read-
267 Write Integrator to Dynamically Coordinate T Helper Cell Fate. *Immunity* **47**, 481-497
268 e487 (2017).
269 9. N. J. Tubo *et al.*, Single naive CD4+ T cells from a diverse repertoire produce different
270 effector cell types during infection. *Cell* **153**, 785-796 (2013).
271 10. M. J. Ploquin, U. Eksmond, G. Kassiotis, B cells and TCR avidity determine distinct
272 functions of CD4+ T cells in retroviral infection. *J Immunol* **187**, 3321-3330 (2011).
273 11. N. Fazilleau, L. J. McHeyzer-Williams, H. Rosen, M. G. McHeyzer-Williams, The
274 function of follicular helper T cells is regulated by the strength of T cell antigen
275 receptor binding. *Nat Immunol* **10**, 375-384 (2009).
276 12. V. Vanguri, C. C. Govern, R. Smith, E. S. Huseby, Viral antigen density and
277 confinement time regulate the reactivity pattern of CD4 T-cell responses to vaccinia
278 virus infection. *Proc Natl Acad Sci U S A* **110**, 288-293 (2013).
279 13. A. Oxenius, M. F. Bachmann, R. M. Zinkernagel, H. Hengartner, Virus-specific MHC-
280 class II-restricted TCR-transgenic mice: effects on humoral and cellular immune
281 responses after viral infection. *Eur J Immunol* **28**, 390-400 (1998).
282 14. L. M. Fahey *et al.*, Viral persistence redirects CD4 T cell differentiation toward T
283 follicular helper cells. *J Exp Med* **208**, 987-999 (2011).
284 15. A. Crawford *et al.*, Molecular and transcriptional basis of CD4(+) T cell dysfunction
285 during chronic infection. *Immunity* **40**, 289-302 (2014).
286 16. J. J. Sabatino, Jr., J. Huang, C. Zhu, B. D. Evavold, High prevalence of low affinity
287 peptide-MHC II tetramer-negative effectors during polyclonal CD4+ T cell responses.
288 *J Exp Med* **208**, 81-90 (2011).
289 17. E. Corse, R. A. Gottschalk, M. Krogsgaard, J. P. Allison, Attenuated T cell responses to
290 a high-potency ligand in vivo. *PLoS Biol* **8**, (2010).
291 18. E. S. Huseby, F. Crawford, J. White, P. Marrack, J. W. Kappler, Interface-disrupting
292 amino acids establish specificity between T cell receptors and complexes of major
293 histocompatibility complex and peptide. *Nat Immunol* **7**, 1191-1199 (2006).
294 19. A. M. Gallegos *et al.*, Control of T cell antigen reactivity via programmed TCR
295 downregulation. *Nat Immunol* **17**, 379-386 (2016).

296 20. C. Kim, T. Wilson, K. F. Fischer, M. A. Williams, Sustained interactions between T cell
297 receptors and antigens promote the differentiation of CD4(+) memory T cells.
298 *Immunity* **39**, 508-520 (2013).
299 21. L. Flatz, A. Bergthaler, J. C. de la Torre, D. D. Pinschewer, Recovery of an arenavirus
300 entirely from RNA polymerase I/II-driven cDNA. *Proc Natl Acad Sci U S A* **103**, 4663-
301 4668 (2006).
302 22. A. Bergthaler *et al.*, Viral replicative capacity is the primary determinant of
303 lymphocytic choriomeningitis virus persistence and immunosuppression. *Proc Natl*
304 *Acad Sci U S A* **107**, 21641-21646 (2010).
305 23. B. M. Sullivan *et al.*, Point mutation in the glycoprotein of lymphocytic
306 choriomeningitis virus is necessary for receptor binding, dendritic cell infection, and
307 long-term persistence. *Proc Natl Acad Sci U S A* **108**, 2969-2974 (2011).
308 24. A. Bergthaler, D. Merkler, E. Horvath, L. Bestmann, D. D. Pinschewer, Contributions
309 of the lymphocytic choriomeningitis virus glycoprotein and polymerase to strain-
310 specific differences in murine liver pathogenicity. *J Gen Virol* **88**, 592-603 (2007).
311 25. X. Liu *et al.*, Alternate interactions define the binding of peptides to the MHC
312 molecule IA(b). *Proc Natl Acad Sci U S A* **99**, 8820-8825 (2002).
313 26. M. Kunzli *et al.*, Long-lived T follicular helper cells retain plasticity and help sustain
314 humoral immunity. *Sci Immunol* **5**, (2020).
315 27. S. S. Iyer *et al.*, Identification of novel markers for mouse CD4(+) T follicular helper
316 cells. *Eur J Immunol* **43**, 3219-3232 (2013).
317 28. R. Andargachew, R. J. Martinez, E. M. Kolawole, B. D. Evavold, CD4 T Cell Affinity
318 Diversity Is Equally Maintained during Acute and Chronic Infection. *J Immunol* **201**,
319 19-30 (2018).
320 29. Y. Dong *et al.*, CD4(+) T cell exhaustion revealed by high PD-1 and LAG-3 expression
321 and the loss of helper T cell function in chronic hepatitis B. *BMC Immunol* **20**, 27
322 (2019).
323 30. Z. Mou *et al.*, Parasite-derived arginase influences secondary anti-Leishmania
324 immunity by regulating programmed cell death-1-mediated CD4+ T cell exhaustion. *J*
325 *Immunol* **190**, 3380-3389 (2013).
326 31. M. Jean Bosco *et al.*, The exhausted CD4(+)CXCR5(+) T cells involve the pathogenesis
327 of human tuberculosis disease. *Int J Infect Dis* **74**, 1-9 (2018).
328 32. C. Yao *et al.*, Single-cell RNA-seq reveals TOX as a key regulator of CD8(+) T cell
329 persistence in chronic infection. *Nat Immunol* **20**, 890-901 (2019).
330 33. F. Alfei *et al.*, TOX reinforces the phenotype and longevity of exhausted T cells in
331 chronic viral infection. *Nature* **571**, 265-269 (2019).
332 34. O. Khan *et al.*, TOX transcriptionally and epigenetically programs CD8(+) T cell
333 exhaustion. *Nature* **571**, 211-218 (2019).
334 35. A. C. Scott *et al.*, TOX is a critical regulator of tumour-specific T cell differentiation.
335 *Nature* **571**, 270-274 (2019).
336 36. H. Seo *et al.*, TOX and TOX2 transcription factors cooperate with NR4A transcription
337 factors to impose CD8(+) T cell exhaustion. *Proc Natl Acad Sci U S A* **116**, 12410-
338 12415 (2019).
339 37. W. Xu *et al.*, The Transcription Factor Tox2 Drives T Follicular Helper Cell
340 Development via Regulating Chromatin Accessibility. *Immunity* **51**, 826-839 e825
341 (2019).

342 38. S. J. Im *et al.*, Defining CD8+ T cells that provide the proliferative burst after PD-1
343 therapy. *Nature* **537**, 417-421 (2016).
344 39. D. T. Utzschneider *et al.*, T Cell Factor 1-Expressing Memory-like CD8(+) T Cells
345 Sustain the Immune Response to Chronic Viral Infections. *Immunity* **45**, 415-427
346 (2016).
347 40. L. A. Vella, R. S. Herati, E. J. Wherry, CD4(+) T Cell Differentiation in Chronic Viral
348 Infections: The Tfh Perspective. *Trends Mol Med* **23**, 1072-1087 (2017).
349 41. N. J. Tubo *et al.*, Single Naive CD4(+) T Cells from a Diverse Repertoire Produce
350 Different Effector Cell Types during Infection. *Cell* **153**, 785-796 (2013).
351 42. N. Fazilleau, L. J. McHeyzer-Williams, H. Rosen, M. G. McHeyzer-Williams, The
352 function of follicular helper T cells is regulated by the strength of T cell antigen
353 receptor binding. *Nat Immunol* **10**, 375-384 (2009).
354 43. R. A. Gottschalk *et al.*, Distinct influences of peptide-MHC quality and quantity on in
355 vivo T-cell responses. *Proc Natl Acad Sci U S A* **109**, 881-886 (2012).
356 44. M. J. Ploquin, U. Eksmond, G. Kassiotis, B cells and TCR avidity determine distinct
357 functions of CD4+ T cells in retroviral infection. *J Immunol* **187**, 3321-3330 (2011).
358 45. K. A. Allison *et al.*, Affinity and dose of TCR engagement yield proportional enhancer
359 and gene activity in CD4+ T cells. *Elife* **5**, (2016).
360 46. X. Tao, S. Constant, P. Jorritsma, K. Bottomly, Strength of TCR signal determines the
361 costimulatory requirements for Th1 and Th2 CD4+ T cell differentiation. *J Immunol*
362 **159**, 5956-5963 (1997).
363 47. N. A. Hosken, K. Shibuya, A. W. Heath, K. M. Murphy, A. O'Garra, The effect of
364 antigen dose on CD4+ T helper cell phenotype development in a T cell receptor-
365 alpha beta-transgenic model. *J Exp Med* **182**, 1579-1584 (1995).
366 48. P. A. Bretscher, G. Wei, J. N. Menon, H. Bielefeldt-Ohmann, Establishment of stable,
367 cell-mediated immunity that makes "susceptible" mice resistant to Leishmania
368 major. *Science* **257**, 539-542 (1992).
369 49. B. L. Lohman, R. M. Welsh, Apoptotic regulation of T cells and absence of immune
370 deficiency in virus-infected gamma interferon receptor knockout mice. *J Virol* **72**,
371 7815-7821 (1998).
372 50. M. Schorer *et al.*, TIGIT limits immune pathology during viral infections. *Nat Commun*
373 **11**, 1288 (2020).
374 51. L. M. Snell *et al.*, Overcoming CD4 Th1 Cell Fate Restrictions to Sustain Antiviral CD8
375 T Cells and Control Persistent Virus Infection. *Cell Rep* **16**, 3286-3296 (2016).
376 52. I. A. Parish *et al.*, Chronic viral infection promotes sustained Th1-derived
377 immunoregulatory IL-10 via BLIMP-1. *J Clin Invest* **124**, 3455-3468 (2014).
378 53. B. Corre *et al.*, Type I interferon potentiates T-cell receptor mediated induction of IL-
379 10-producing CD4(+) T cells. *Eur J Immunol* **43**, 2730-2740 (2013).
380 54. M. Saraiva *et al.*, Interleukin-10 production by Th1 cells requires interleukin-12-
381 induced STAT4 transcription factor and ERK MAP kinase activation by high antigen
382 dose. *Immunity* **31**, 209-219 (2009).
383 55. J. R. Teijaro *et al.*, Persistent LCMV infection is controlled by blockade of type I
384 interferon signaling. *Science* **340**, 207-211 (2013).
385 56. E. B. Wilson *et al.*, Blockade of chronic type I interferon signaling to control
386 persistent LCMV infection. *Science* **340**, 202-207 (2013).
387 57. K. Richter, G. Perriard, A. Oxenius, Reversal of chronic to resolved infection by IL-10
388 blockade is LCMV strain dependent. *Eur J Immunol* **43**, 649-654 (2013).

389 58. R. J. Martinez, R. Andargachew, H. A. Martinez, B. D. Evavold, Low-affinity CD4+ T
390 cells are major responders in the primary immune response. *Nat Commun* **7**, 13848
391 (2016).
392 59. M. Battegay, [Quantification of lymphocytic choriomeningitis virus with an
393 immunological focus assay in 24 well plates]. *ALTEX* **10**, 6-14 (1993).
394 60. J. J. Moon *et al.*, Tracking epitope-specific T cells. *Nat Protoc* **4**, 565-581 (2009).
395

396 **Material & Methods**

397

398 *Viruses*

399 Virus rescue was performed as described previously using the pol-I/pol-II-driven
400 reverse genetic system for LCMV (*21*). Single amino acids changes of the GP61-
401 epitope were introduced by site directed mutagenesis of the previously described pI-
402 S-WE-GP rescue plasmid (*21*). This plasmid encodes the nucleoprotein (NP) of the
403 LCMV Armstrong strain *on cis* with the glycoprotein (GP) of LCMV WE. Additionally,
404 the LCMV Armstrong specific D63K mutation was introduced into the GP61-coding
405 sequence of the WE-GP gene matching the LCMV Armstrong / Clone-13 amino acid
406 sequence of the GP61 peptides employed in the T cell activation assay. The resulting
407 S-rescue plasmids were combined either a plasmid expressing either the Armstrong
408 or the Clone-13 L segment in order to generate acute and chronic variants
409 respectively. The presence of the desired mutations in the viral genomes was verified
410 by sanger sequencing of RT-PCR amplicons generated with the OneStep RT-PCR-kit
411 (Qiagen) using LCMV WE GP-specific primers (GATTGCGCTTTCCTCTAGATC and
412 TCAGCGTCTTTTCCAGATAG). Viral RNA was extracted from cell culture
413 supernatants using the Direct-zol RNA MicroPrep kit (Zymo Research). Virus titer were
414 determined by immunofocus assay as described on NIH/3T3 cells (*59*).

415

416 *Viral growth kinetics*

417 To determine viral replication capacities, BHK21 cells were seeded 24 hours prior to
418 infection with a MOI of 0.01. Supernatant was collected at indicated time points and
419 replaced with fresh culture medium.

420

421 *Mice and Animal experiments*

422 Mice were bred and housed under specific pathogen-free conditions at the University
423 Hospital of Basel according to the animal protection law in Switzerland. For all
424 experiments, male or female sex-matched mice were used that were at least 6 weeks
425 old at the time point of infection. The following mouse strains were used: C57BL/6
426 CD45.2, SMARTA Ly5.1, CD74$^{-/-}$. Mice were injected with intraperitoneal injection of
427 2x10^{5} FFU for Armstrong variants or via intravenous injection of 2x10^{6} FFU for Clone-
428 13 variants.

429

430 *NICD-protector*

431 Mice were intravenously (i.v.) injected with 12.5µg homemade ARTC2.2-blocking
432 nanobody s+16 (NICD-protector) at least 15 minutes prior to organ harvest.

433

434 *Adoptive cell transfer*

435 Single-cell suspensions of cells were prepared from lymph nodes by mashing and
436 filtering through a 100µm strainer. Naïve Smarta cells were enriched using Naïve CD4
437 T cell isolation kit (StemCell). 1x10^{4} SMARTA Ly5.1 cells were adoptively transferred
438 into Ly5.2 recipients via intravenous injection as previously described (*60*).

439

440 *Flow Cytometry*

441 Spleens were removed and single-cell suspensions were generated by mashing and
442 filtering the spleens through a 100µm strainer followed by erythrocytes lysing using
443 Ammonium-Chloride-Potassium (ACK) lysis buffer. SMARTA and endogenous LCMV-
444 specific CD4 T cells were analyzed using IAb:NP309-328 (PE) or IAb:GP66-77 (APC)
445 (provided by NIH tetramer core) tetramer. Following staining for 1 hour at room

446 temperature in the presence of 50nM Dasatinib, tetramer-binding cells were enriched
447 using magnetic beads and counted as previously published (*60*). Surface combined
448 with viability staining was performed for 30min on ice. For transcription factor staining,
449 fixation and permeabilization was performed according to the Foxp3/Transcription
450 Factor staining kit (eBioscience). Samples were analyzed on Fortessa LSR II or Canto
451 II cytometers (BD Biosciences) followed by data analysis with FlowJo X software
452 (TreeStar). $CD4^+$ T cells were pre-gated on lymphocytes in FSC/SSC, dump-, live
453 $CD4^+$ cells and then further gated on $CD44^+$ $Tetramer^-$ to assess the $CD44^+$
454 compartment, $CD44^+$ $CD45.1^+$ $GP66^+$ for SMARTA and $CD44^+$ $NP309^+$ for NP-specific
455 cells.
456 The following antibodies were used: CD4 (BUV496, GK1.5, BD, #564667; APC
457 eFluor780, GK1.5, eBioscience, #47-0041-82), CD11b (PE-Cy5, M1/70, BioLegend,
458 #101222), B220 (PE-Cy5, RA3-6B2, BioLegend, #103210, PE-Cy7, RA3-6B2,
459 BioLegend, #103222), CD11c (PE-Cy5, N418, BioLegend, #117316; AF647, N418,
460 BioLegend, #117312), CD44 (BUV395, IM7, BD), CD45.1 (FITC, A20, BD, #553775;
461 APC, A20, eBioscience, #17-0453-82), CD45.2 (APC-Fire, 104, BioLegend,
462 #109852), CD69 (PE, H1.2F3, eBioscience), CD62L (APC, MEL-14, BD, #553152),
463 PSGL-1 (BV605, 2PH1, BD, #740384), PD1 (BV785, 29F.1A12, BioLegend,
464 #135225), Vα2 TCR (PE, B20.1, eBioscience, #12-5812-82; FITC, B20.1,
465 eBioscience, #11-5812-82), Vβ8.3 TCR (FITC, 1B3.3, BD, #553663), F4/80 (PE-Cy5,
466 BM8, BioLegend, #123112), I-Ab (PE, AF6-120.1, BD, #553552), FR4 (PE-Cy7, 12A5,
467 BioLegend, #125012), Ly6C (BV510, HK1.4, BioLegend, #128033), Bcl6 (BV421,
468 K112-91, BD, #563363), T-bet (BV711, 4B10, BioLegend, #644820), TOX (PE,
469 TXRX10, eBioscience, #12-6502-82), Lag3 (BV421, C9B7W, BioLegend, #125221),

470 TCF1 (AF700, 812145, R&D Systems, #FAB8224N), Zombie Fixable Viability Dye
471 (Zombie Red, BioLegend, #423110).
472
473 *CD69 SMARTA activation assays*
474 Serial dilutions of the GP61-wt peptide or APLs were plated. $5x10^5$ Ly5.2 Splenocytes
475 and $1x10^5$ Ly5.1 SMARTA cells per well were added to the dilution series, stimulated
476 overnight at 37°C, and subsequently stained and analyzed at the flow cytometer.
477
478 *MHC-II out-competition assays*
479 $CD74^{-/-}$ splenocytes were cultured with a custom made GP61-FITC at a fixed
480 concentration of $1x10^{-6}$ M and various serial dilutions of GP61-wt or APLs for 4 hours
481 at 37°C. After stimulation, the cells were stained and analyzed at the flow cytometer.
482 The FITC-labelled GP61 peptide was custom made by Eurogentec.
483
484 *Statistical analysis*
485 Geometric mean was used to determine the mean fluorescence intensity (MFI) and
486 values were normalized to the mean of the control group from each experiment before
487 data was pooled. Pooled and normalized MFIs are referred to as relative MFI. EC_{50}
488 values were calculated using a sigmoidal dose-response fit in GraphPad Prism
489 (version 8). For statistical analysis of one parameter between two groups, unpaired
490 two-tailed Student's t-tests were used to determine statistical significance. To compare
491 one parameter between more than two groups, one-way analysis of variance
492 (ANOVA) was used followed by Turkey's post-test for multiple comparisons. P values
493 are indicated on the graphs. Data was analyzed using GraphPad Prism software
494 (version 8).